Quadruplex ligands may act as molecular chaperones for tetramolecular quadruplex formation

Anne De Cian[1] & Jean-Louis Mergny[1]*

Supplementary Material

February 3, 2007

SUPPLEMENTARY METHODS

Circular dichroism

Formation of a parallel quadruplex was confirmed by circular dichroism (**Supplementary Figure S1A**) on a Jasco J-810 CD spectrophotometer, thermostated with Peltier effects. For thermal denaturation, CD scans (1 accumulation from 320 to 235 nm at 200 nm/min, in a 1 cm path length cell, with a data pitch of 1 nm and a response of 1 s) were recorded at regular time/temperature intervals, every 120s for a heating rate of 0.5°C/min (increase of 1°C every 2 min, scanning after 1min30 for temperature stabilization), and plots of ellipticity *vs*. temperature were generated for 260nm. Most melting curves recorded by heating a preformed quadruplex do not correspond to equilibrium melting curves (hysteresis phenomenon) and the "T_m" deduced from these experiments depends on the heating rate. In order to distinguish it from the true thermodynamic T_m, we will call this value $T_{1/2}$. The heating rate applied for CD melting experiments may be a little high for accurate temperature stabilization during the scans, but it was chosen in order to be in agreement with the $T_{1/2}$ found using absorbance

(without any ligand); this may explain the 1-2°C difference between the $T_{1/2}$ values obtained by CD and absorbance experiments.

Fluorescence titrations

Fluorescence spectra were recorded at 4°C in 3ml quartz cuvets containing 10 mM lithium cacodylate pH 7.2 and 110mM KCl. The emission of 0.6µM ligand 360A (excitation at 320 nm) was measured after successive additions of G-quadruplex $[PO_4\text{-}TG_3T]_4$ (preformed at higher concentration (1440 µM) in the same buffer), or of single-stranded $PO_4\text{-}TG_3T$ (in ddH_2O and freshly heat denaturated). Considering our study and the weak concentration of ligand used for the titration we assumed that the induction of tetramolecular species from the single-stranded oligonucleotide was negligible during the time course of the experiment.

Supplementary Table 1 : Properties of the DNA ligands tested:

Compound	**MW** [a]	**Charge**	**ΔT_m (K^+)** [b]	**ΔT_m (Na^+)** [b]	**Kd (M)** [c]	**n** [d]	**References** [e]
360A	449.5	+2	30 °C	25.1 °C	6.4×10^{-8}	2	(1-3)
Telomestatin	582.5	0	22.8 °C	23.6 °C	nd	2	(4-6)
TMPyP4	678.8	+4	27.4 °C	21 °C	1.4×10^{-5}	2-4	(6-10)
Ethidium	314.4	+1	0.7 °C	1.1 °C	$6.7 \times 10^{-6*}$	1-2	(11-13)
307A	449.5	+2	32°C	25°C	9.0×10^{-9}	2	(1-3)
12459	410.5	+2	26.5°C	15.6°C	nd	2	(14)
BRACO19	595.8	+2	22°C	11°C	6.3×10^{-8}	2	(15)
BSU1051	608.8	+2	9°C	3.5°C	nd		(16)
PIPER	614.7	(+2)	23°C	16°C	nd	1-2	(17-19)

[a] : Not taking into account possible counterions.

[b] : Experimental conditions as in De Cian *et al.* (20) with the intramolecular G-quadruplex FAM-GGG(TTAGGG)$_3$-TAMRA for 1μM of ligand. Values are given with a precision of 1°C.

[c] : K_d Dissociation constant of the ligand for 22AG quadruplexe except when notified by * (Ethidium – T_4G_4) . Note that the experimental conditions used may vary.

[d]: Stoichiometry (number of binding sites per quadruplex) found (by Mass spectrometry or titrations) or predicted (by molecular modeling).

[e] : Examples of articles where the interaction of this molecule has been tested on quadruplex DNA; this list is not exhaustive.

Supplementary Figure S1: Formulae of the duplex/G-quadruplex ligands used in this study.

Supplementary Figure S2: Interaction of 360A and $[PO_4\text{-}TG3T]_4$: CD spectra and melting experiment

A: CD spectra of PO_4-TG_3T at 25°C in 10mM lithium cacodylate pH 7.2, 110mM KCl for various conditions: black line: PO_4-TG_3T 20µM (G-quadruplex preformed at 1440 µM in 10mM Lithium Cacodylate pH 7.2, 110mM KCl at 4°C over a week); green triangles: PO_4-TG3T 20µM (Preformed G-quadruplex) + 360A 5µM ; Light blue triangles: PO_4-TG_3T 20µM incubated overnight at 4°C with 5µM 360A; dark blue circles: PO_4-TG_3T 20 µM incubated 2 days at 4°C with 10 µM 360A ; red triangles : PO_4-TG_3T 20µM single-stranded.

B: Thermal denaturation of PO_4-TG_3T preformed G-quadruplex alone or induced G-quadruplex at 20 µM (strand concentration) by 360A after O/N incubation with 5 or 10µM 360A. CD signal is recorded at 260nm and normalized between 0 and 1: PO_4-TG_3T 20µM alone (preformed at higher concentration)(black diamonds) or induced with 5µM (light blue triangles) or 10 µM (dark blue triangles) 360A.

C: CD spectra as a function of temperature for the Phosphorylated TG_3T oligonucleotide alone (left) or in the presence of 10 µM 360A (right). The arrows show the direction of temperature increase.

Supplementary Figure S3: Isothermal differential spectra

A: Normalized isothermal difference (initial unfolded state minus final, associated state) for

the TG_3T oligonucleotide 5'OH (black circles) or 5'phosphate (red triangles). Experimental conditions : spectra of TG_3T (100 µM) and PO_4-TG_3T (300 µM) in 10 mM lithium cacodylate (pH 7.2), KCl 110 mM buffer are recorded at 4°C immediately after heat denaturation (*unfolded* state) and after overnight kinetics at 4°C (*associated* state).

B: Normalized isothermal difference (initial unfolded state minus final, associated state) for the TG_3T oligonucleotide alone (black circles) or in the presence of various concentrations of ligand (blue curves). Note the positive signal in the visible region, showing that the absorbance properties of the dyes are affected when bound to the quadruplex. Contribution of ligand binding in the UV region modifies the amplitude of the main peaks without changing their characteristic wavelengths. The overall architecture is likely to be a G-quadruplex as also suggested by circular dichroism spectra. Experimental conditions: spectra of TG_3T at 100 µM when alone, or at 10 µM in presence of 360A at 2.5, 5 and 10 µM are recorded at 4°C, in 10 mM lithium cacodylate (pH 7.2), KCl 110 mM buffer, immediately after heat denaturation (*unfolded* state) and after overnight kinetics at 4°C (*associated* state).

Supplementary Figure S4: Comparison of $[TG3T]_4$ and $[PO_4\text{-}TG3T]_4$ association and dissociation

A: Gel quantification of the single-stranded fraction using UV-shadow (red triangles: TG_3T (**Fig. 3E** and **Fig. 2**) ; grey squares: PO_4-TG_3T) or radioactive detection (black diamonds: PO_4-TG_3T) ; k_{on} values are calculated using a fourth order model (21).

B: Effect of KCl concentration on association rate of 5'-OH (red circle) and 5' phosphate (black diamonds) oligonucleotides.

C: Effect of KCl concentration on thermal stability ($T_{1/2}$ value) of 5'-OH (red circle) and 5' phosphate (black diamonds) G-quadruplexes. G-quadruplexes were preformed at high

concentration (800µM) over night in Lithium cacodylate 10 mM pH 7.2 and 110 mM (for 30 mM, 50 mM and 110 mM experiments), 300 mM or 500 mM KCl. The corresponding buffer was then added to reach the convenient KCl final concentration and about 20µM in DNA (strand concentration).

Supplementary Figure S5: Interaction of 360A with $[PO_4\text{-}TG3T]_4$: fluorescence quenching.

Fluorescence titration of 360A by $[PO_4\text{-}TG_3T]_4$ or $PO_4\text{-}TG_3T$ at 4°C in Lithium Cacodylate pH 7.2, KCl 110mM. Left panel: 360A (0.6µM) fluorescence spectra for excitation at 320nm in presence of increasing amounts of $[PO_4\text{-}TG_3T]_4$ (G-quadruplex preformed at high concentration in the same buffer); central panel: 360A (0.5µM) fluorescence spectra for excitation at 320nm in presence of increasing amounts of single stranded $PO_4\text{-}TG_3T$; right panel: integrated fluorescence normalized to the fluorescence of 360A alone as a function of $PO_4\text{-}TG_3T$ molar equivalent (lower X-axis ; blue circles) or $[PO_4\text{-}TG_3T]_4$ molar equivalent (upper X-axis ; black triangles).

Supplementary Figure S6: Effect of 360A on other sequences.

A: Association kinetics of $[T_2AG_3]_4$ incubated at 4°C at a strand concentration of 200µM or 100 µM in absence or presence of 360A at 10 and 25 µM.

B: Association kinetics of $[T_2AG_3T]_4$ incubated at 4°C at a strand concentration of 100 µM in absence or presence of 360A at 10, 25 and 50 µM.

Both kinetics are performed in 10 mM Lithium Cacodylate pH 7.2, 110 mM KCl buffer. Products are resolved by a 20% native acrylamide gel electrophoresis performed at 4°C

containing 1X TBE and 20 mM KCl, and detected by UV shadow at 254 nm.

C: lane 1-5: Association of $[T_2G_5T_2]_4$ at 100 µM strand concentration in 10mM Lithium cacodylate pH 7.2, 110 mM NaCl buffer after 1hour of incubation at 4°C in presence of various concentration of 360A. Lane 6-10: preformed G-quadruplex $[T_2G_5T_2]_4$ in absence or presence of various concentrations of 360A. The gel-shift of the G-quadruplex induced by the ligand 360A (lanes 2-5) is nearly identical to the one of the preformed G-quadruplex bound to 360A (lane 7-10).

References:

1. Lemarteleur, T., Gomez, D., Paterski, R., Mandine, E., Mailliet, P. and Riou, J.-F. (2004) Stabilization of the c-myc gene promoter quadruplex by specific ligands inhibitors of telomerase. *Biochem. Biophys. Res. Com.*, **323**, 802-808.
2. Pennarun, G., Granotier, C., Gauthier, L.R., Gomez, D., Hoffschir, F., Mandine, E., Riou, J.F., Mergny, J.L., Mailliet, P. and Boussin, F.D. (2005) Apoptosis related to telomere instability and cell cycle alterations in human glioma cells treated by new highly selective G-quadruplex ligands. *Oncogene*, **24**, 2917-2928.
3. Granotier, C., Pennarun, G., Riou, L., Hoffschir, F., Gauthier, L.R., DeCian, A., Gomez, D., Mandine, E., Riou, J.F., Mergny, J.L. *et al.* (2005) Preferential binding of a G-quadruplex ligand to human chromosome ends. *Nucl Acid Res*, **33**, 4182-4190.
4. Shin-ya, K., Wierzba, K., Matsuo, K., Ohtani, T., Yamada, Y., Furihata, K., Hayakawa, Y. and Seto, H. (2001) Telomestatin, a novel telomerase inhibitor from Streptomyces anulatus. *J. Am. Chem. Soc.*, **123**, 1262-1263.
5. Kim, M.Y., Vankayalapati, H., Shin-ya, K., Wierzba, K. and Hurley, L.H. (2002) Telomestatin, a potent telomerase inhibitor that interacts quite specifically with the human telomeric intramolecular G-quadruplex. *J. Am. Chem. Soc.*, **124**, 2098-2099.
6. Kim, M.Y., Gleason Guzman, M., Izbicka, E., Nishioka, D. and Hurley, L.H. (2003) The different biological effects of telomestatin and TMPyP4 can be attributed to their selectivity for interaction with intramolecular or intermolecular G-quadruplex structures. *Cancer Res.*, **63**, 3247-3256.
7. Izbicka, E., Wheelhouse, R.T., Raymond, E., Davidson, K.K., Lawrence, R.A., Sun, D.Y., Windle, B.E., Hurley, L.H. and VonHoff, D.D. (1999) Effects of cationic porphyrins as G-quadruplex interactive agents in human tumor cells. *Cancer Res.*, **59**, 639-644.
8. Han, F.X.G., Wheelhouse, R.T. and Hurley, L.H. (1999) Interactions of TMPyP4 and TMPyP2 with quadruplex DNA. Structural basis for the differential effects on telomerase inhibition. *J. Am. Chem. Soc.*, **121**, 3561-3570.
9. Han, H., Langley, D.R., Rangan, A. and Hurley, L.H. (2001) Selective Interactions of Cationic Porphyrins with G-Quadruplex Structures. *J. Am. Chem. Soc.*, **123**, 8902-8913.

10. Wei, C., Jia, G., Yuan, J., Feng, Z. and Li, C. (2006) A spectroscopic study on the interactions of porphyrin with G-quadruplex DNAs. *Biochemistry*, **45**, 6681-6691.
11. Guo, Q., Lu, M., Marky, L.A. and Kallenbach, N.R. (1992) Interaction of the dye ethidium bromide with DNA containing guanine repeats. *Biochemistry*, **31**, 2451-2455.
12. Koeppel, F., Riou, J.F., Laoui, A., Mailliet, P., Arimondo, P.B., Labit, D., Petigenet, O., Hélène, C. and Mergny, J.L. (2001) Ethidium derivatives bind to G-quartets, inhibit telomerase and act as fluorescent probes for quadruplexes. *Nucleic Acids Res.*, **29**, 1087-1096.
13. Rosu, F., Pauw, E.D., Guittat, L., Alberti, P., Lacroix, L., Mailliet, P., Riou, J.-F. and Mergny, J.-L. (2003) Selective interaction of ethidium derivatives with quadruplexes. *Biochemistry*, **42**, 10361-10371.
14. Riou, J.F., Guittat, L., Mailliet, P., Laoui, A., Petigenet, O., Megnin-Chanet, F., Hélène, C. and Mergny, J.L. (2002) Cell senescence and telomere shortening induced by a new series of specific G-quadruplex DNA ligands. *Proc. Natl. Acad. Sci. USA*, **99**, 2672-2677.
15. Read, M., Harrison, R.J., Romagnoli, B., Tanious, F.A., Gowan, S.H., Reszka, A.P., Wilson, W.D., Kelland, L.R. and Neidle, S. (2001) Structure-based design of selective and potent G quadruplex-mediated telomerase inhibitors. *Proc. Natl. Acad. Sci. USA*, **98**, 4844-4849.
16. Sun, D., Thompson, B., Cathers, B.E., Salazar, M., Kerwin, S.M., Trent, J.O., Jenkins, T.C., Neidle, S. and Hurley, L.H. (1997) Inhibition of human telomerase by a G-quadruplex-interactive compound. *J. Med. Chem.*, **40**, 2113-2116.
17. Han, H.Y., Cliff, C.L. and Hurley, L.H. (1999) Accelerated assembly of G-quadruplex structures by a small molecule. *Biochemistry*, **38**, 6981-6986.
18. Kern, J.T., Thomas, P.W. and Kerwin, S.M. (2002) The relationship between ligand aggregation and G-quadruplex DNA selectivity in a series of 3,4,9,10-perylenetetracarboxylic acid diimides. *Biochemistry*, **41**, 11379-11389.
19. Kerwin, S.M., Chen, G., Kern, J.T. and Thomas, P.W. (2002) Perylene diimide G-quadruplex DNA binding selectivity is mediated by ligand aggregation. *Bioorg Medicinal Chem Letter*, **12**, 447-450.
20. De Cian, A., Guittat, L., Kaiser, M., Saccà, B., Amrane, S., Bourdoncle, A., Alberti, P., Teulade-Fichou, M.P., Lacroix, L. and Mergny, J.L. (2007) Fluorescence-based melting assays for studying quadruplex ligands. *Methods*, **in press**.
21. Mergny, J.L., De Cian, A., Ghelab, A., Saccà, B. and Lacroix, L. (2005) Kinetics of tetramolecular quadruplexes. *Nucleic Acids Res.*, **33**, 81-94.

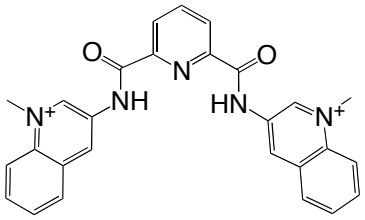

360A

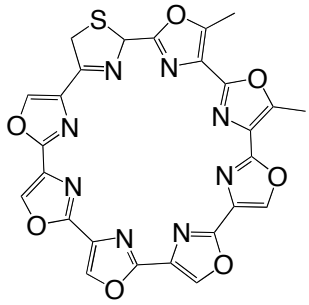

Telomestatin

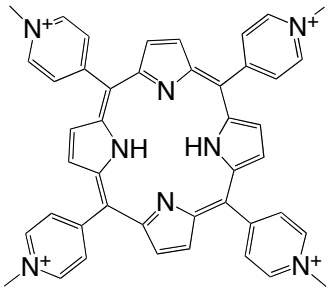

TMPyP4

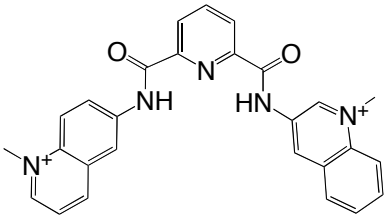

307A

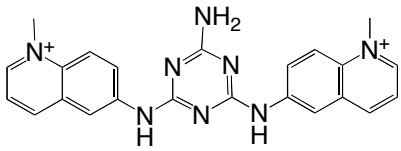

12459

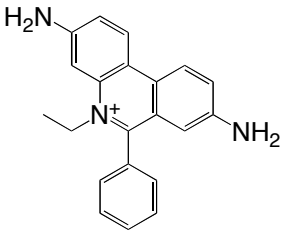

EtBr

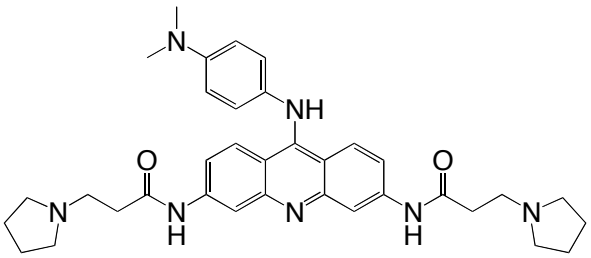

BRACO19

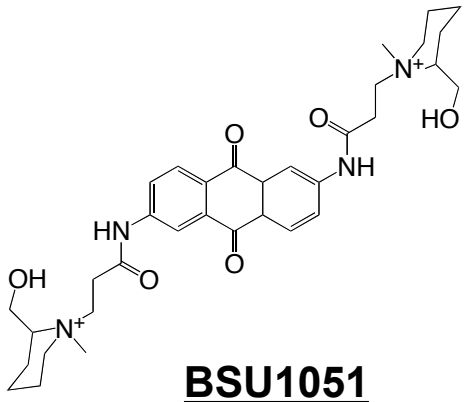

BSU1051

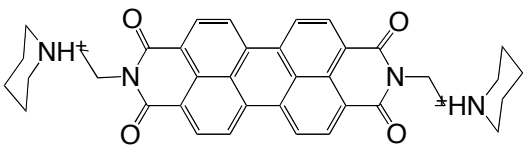

PIPER

Supplementary Figure S1

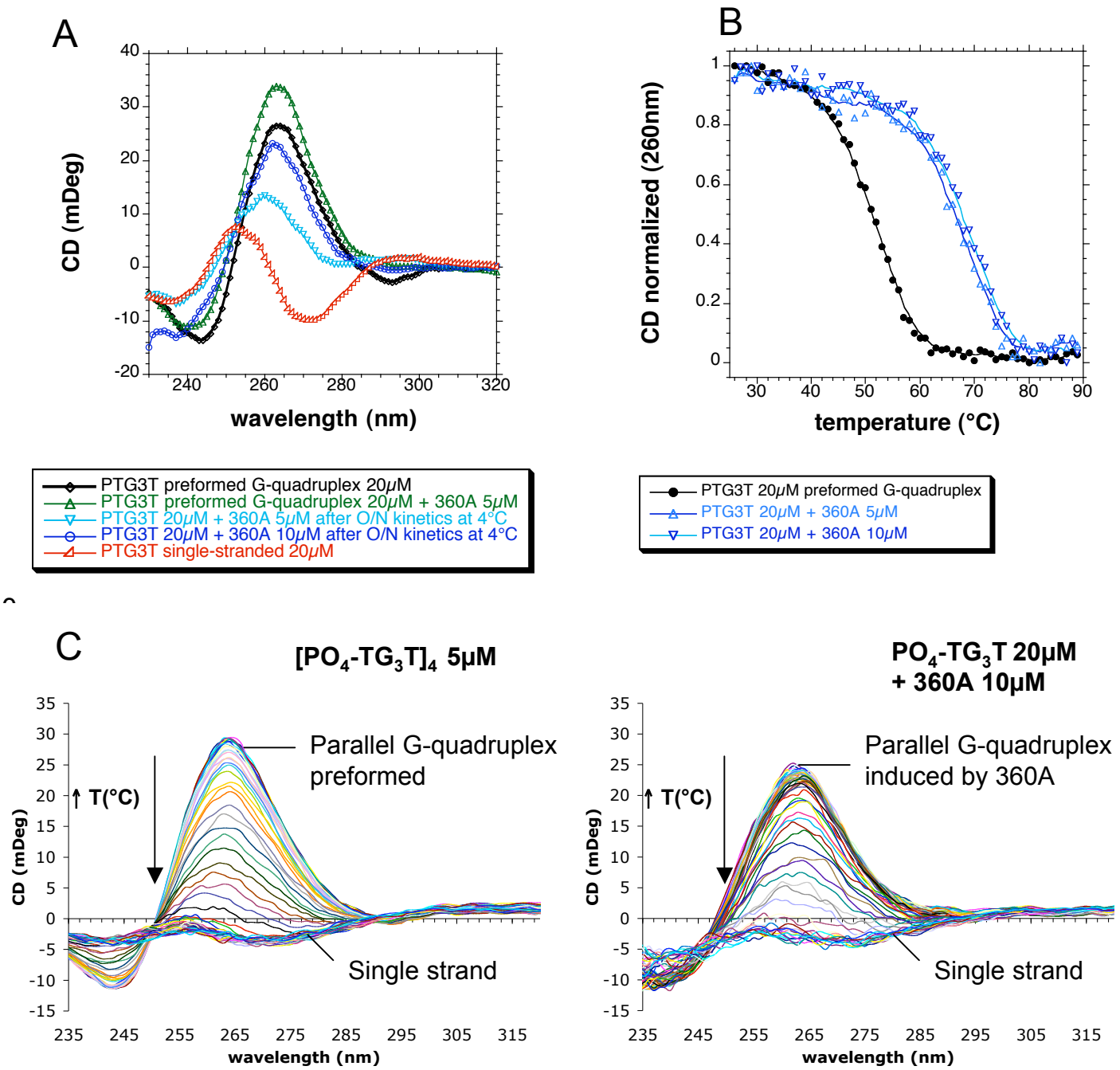

Supplementary Figure S2

A

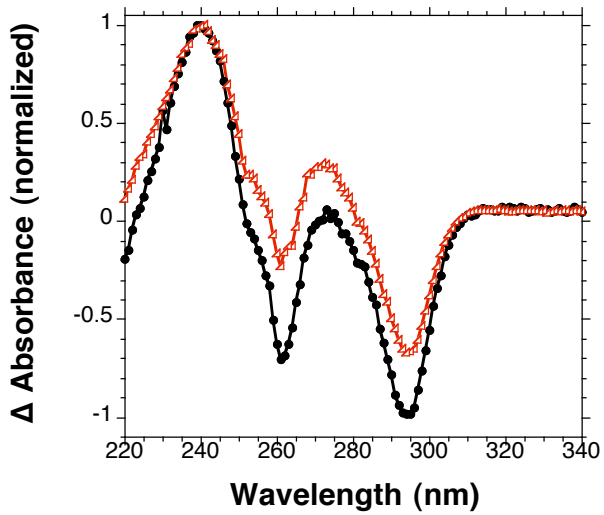

B

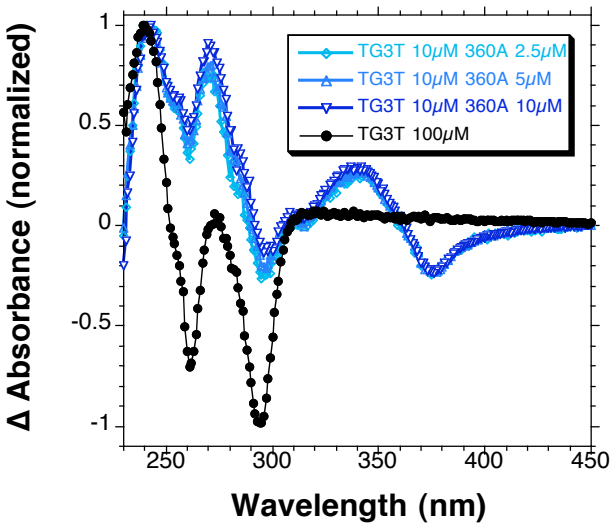

Supplementary Figure S3

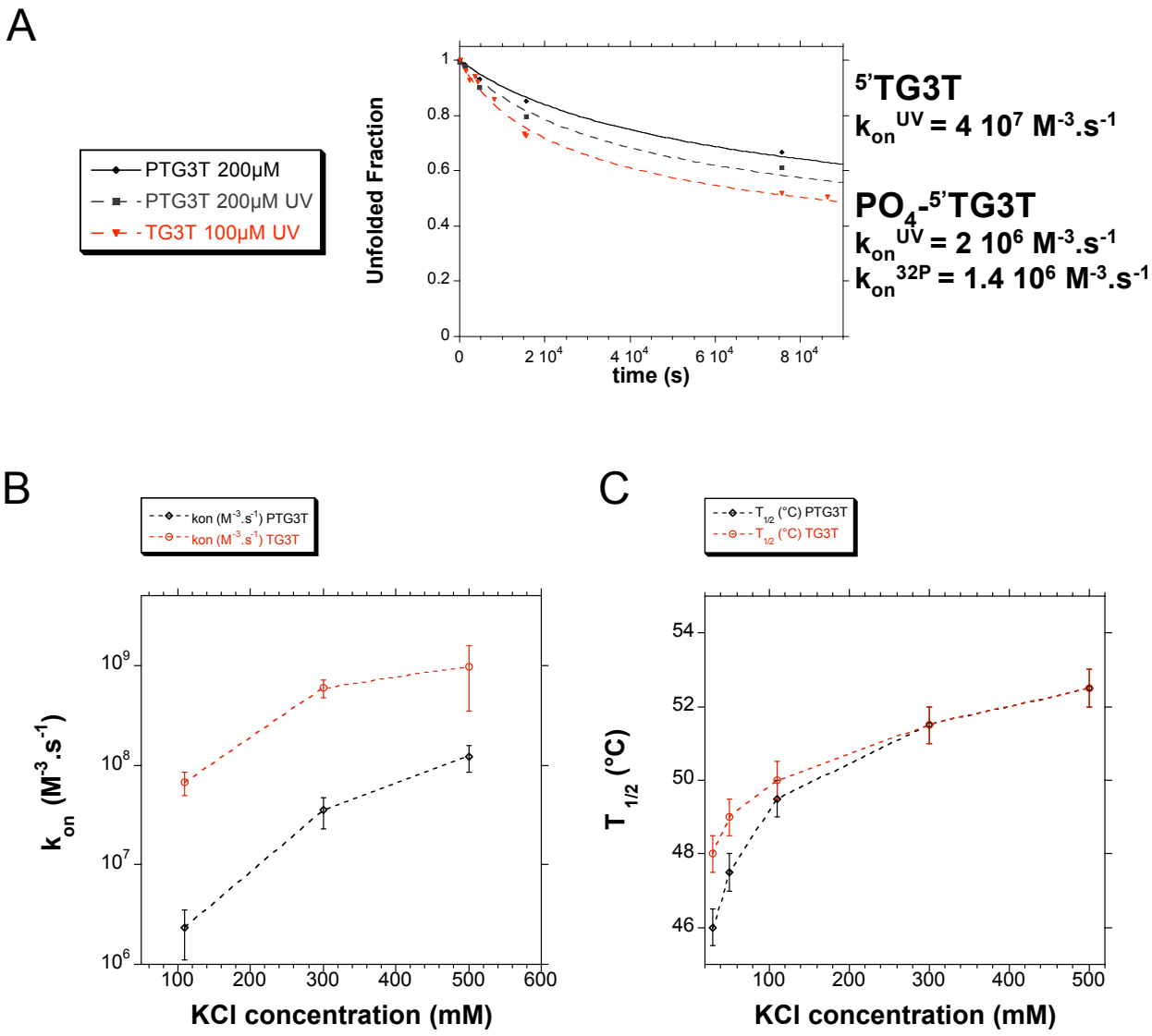

Supplementary Figure S4

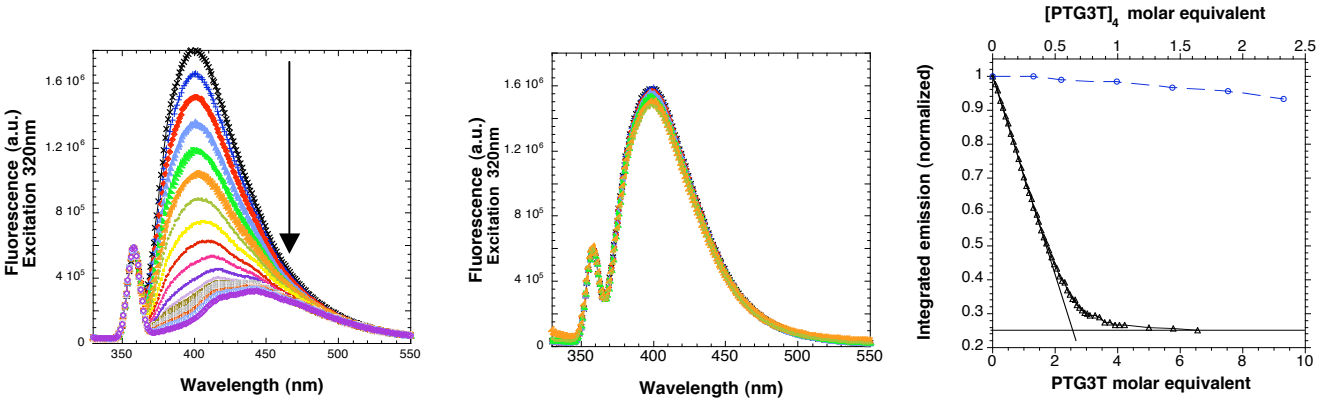

Supplementary Figure S5

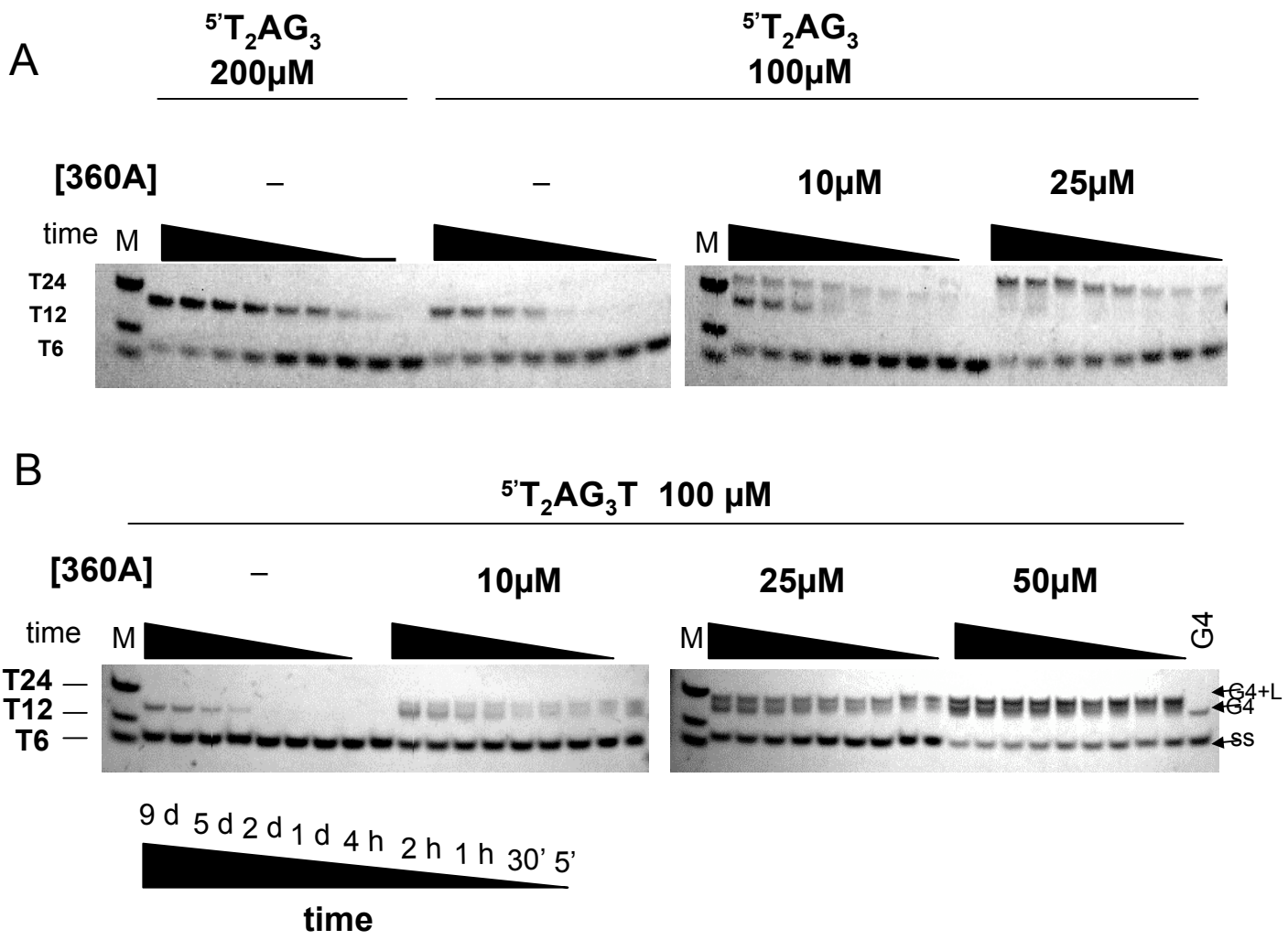

Supplementary Figure S6